Improvements in the Simulation of Orientation in Injection Molding of Short Fiber Thermoplastic Composites

Gregorio M. Vélez-García[a], Syed M. Mazahir[b], Peter Wapperom[c], and Donald G. Baird[b]

[a]*Macromolecular Science and Engineering Department, Virginia Tech, Blacksburg, VA 24061*
[b] *Chemical* Engineering *Department, Virginia Tech, Blacksburg, VA 24061*
[c] *Mathematics Department, Virginia Tech, Blacksburg, VA 24061*

Abstract

The mechanical properties of injection molded short-fiber reinforced thermoplastic composite parts are highly dependent on the orientation distribution of the fibers. A simulation tool capable of predicting fiber orientation accurately as a function of mold design and processing conditions is required as the predicted fiber orientation capabilities in commercial software show large discrepancies when compared with experimentally measured orientation. In this work a two dimensional coupled Hele-Shaw approximation for predicting the flow-induced orientation of glass fibers in injection molded composite parts is presented. In addition to coupling the stresses to fiber orientation for a highly concentrated short glass fiber PBT suspension, the model considers the slowdown of the evolution of orientation due to fiber interaction. Material parameters in the model are determined from basic rheometry rather than using data from injection molding experiments. The equation of motion coupled with stress equations are discretized using the discontinuous Galerkin Finite Element Method. Flow simulations are performed using a measured orientation profile at the gate instead of random orientation assumed in previous studies. Finally, the evolution of fiber orientation in the cavity is determined experimentally using a modified version of the method of ellipses and results are compared against the predicted values of orientation. The fiber orientation predicted in the entry region and the core layer structure at the end of fill region are now in closer agreement with the experimental values, but there are still some discrepancies.

Introduction

Fiber reinforced thermoplastic made by injection molding is an attractive technology to develop lightweight, high-performance materials. The lightweight molded composites consist of a polymeric matrix reinforced with fibers because of the excellent mechanical properties obtained in the final product, the high throughput, and the cost reduction. The desired properties are only obtained when the orientation of the fibers in the direction of mechanical interest is met. However, the fiber orientation varies through the part as a consequence of flow within the mold during the forming; a concept called flow induced orientation. The fibers considered here are short glass fibers defined as fibers with high aspect ratio (a_r > 30) and absolute length below 1 mm.

Optimization of the technology requires a prediction tool using a computer model capable of designing the correct molding machinery, molding and processing conditions, and consistently controlling fiber orientation. The actual capabilities of simulations are unable to make a quantitative prediction of the orientation due to several limitations in the modeling and numerical techniques used to solve the system of equations. Some of these limitations are the use of models which ignore the fiber interactions (Jeffery model), or account for them in a concentration below the commercial interest (Folgar- Tucker model [1]), or ignore the viscoelastic effects of the polymer, and use a decoupled approach to solve the system of equations.

This paper develops a 2D solution for a coupled flow and fiber orientation using the Hele-Shaw (HS) approximation, which is the typical method of flow description in commercial simulators. The material behavior is modeled using a modified version of Folgar-Tucker model [2] and a Newtonian model for the polymer matrix, with parameters determined from simple flow rheology. The modification in the Folgar-Tucker accounts for the slow-down in the fiber motion due to inter-particle interaction occurring in highly concentrated fiber suspension. The objective of this work is to develop an accurate numerical tool capable of predicting the flow-induced orientation of glass fiber in a commercial range of concentrations using a coupled approach.

Governing Equations

The HS flow approximation for an isothermal flow in a center gated disk is described by

$$\frac{1}{r}\frac{\partial}{\partial r}\left(hr\overline{v}_r\right)=0 \qquad (1)$$

$$-\frac{\partial p}{\partial r}+2\eta\frac{\partial^2 v_r}{\partial z^2}+\frac{1}{r}\frac{\partial}{\partial r}\left(rT_{rr}\right)+\frac{\partial T_{zr}}{\partial z}-\frac{T_{\theta\theta}}{r}=0 \qquad (2)$$

where r represents the radial or flow direction, z the gapwise direction, h the half gap width and $\overline{v}_r$ the average radial velocity along the gapwise coordinate, p the pressure, T_{ij} the fiber-contribution to the extra-stress tensor components. These equations are supplemented by the typical boundary conditions for pressure and velocity.

The hydrodynamic extra-stress model is used to represent the fiber-contribution and is defined as

$$\mathbf{T}=\nu\zeta_{str}\left(\left(\nabla\mathbf{v}\right)^T+\nabla\mathbf{v}\right):\mathbf{R_4} \qquad (3)$$

where ν represents the fiber concentration, , ζ_{str} the viscous drag, $\mathbf{A}$ and $\mathbf{R_4}$ the second and fourth order orientation tensor, respectively. R_4 can be expressed in terms of a quadratic closure:

$$\mathbf{R_4}=\mathbf{AA} \qquad (4)$$

The evolution of the second order orientation tensor is governed by:

$$\frac{\partial\mathbf{A}}{\partial t}+\mathbf{v}\bullet\nabla\mathbf{A}=\alpha\left[\left(\nabla\mathbf{v}\right)^T\bullet\mathbf{A}+\mathbf{A}\bullet\left(\nabla\mathbf{v}\right)-2\left(\left(\nabla\mathbf{v}\right)^T+\nabla\mathbf{v}\right):\mathbf{R}_4 -6C_I II\left(\mathbf{A}-\frac{1}{3}\boldsymbol{\delta}\right)\right] \qquad (5)$$

where α represents the slip parameter, C_I the interaction coefficient and II the magnitude of the rate of deformation tensor. The inter-fiber interactions in a semi-dilute and concentrated regime are represented by the last term and the slip parameter in Eq. (5), respectively. With α=1 and C_I =0, Eq. (5) reduces to the Jeffery model, which only accounts for the kinematic effects typical in dilute suspensions.

The second order orientation tensor represents an average orientation of all fibers in a particular region. Experimentally it is computed by

$$A_{ij}=p_i p_j \qquad (6)$$

where p_i and p_j are components of the vector of orientation. They are defined by

$$p_1=\sin\theta\cos\phi \quad p_2=\sin\theta\sin\phi \quad p_3=\cos\theta \qquad (7)$$

where ϕ and θ are the in-plane and out-of-plane angles.

Problem Description and Numerical Methods

Two 75% short shot center-gated disk of 30wt% short glass fiber PBT with average mass of 18.06, average internal diameter (d_i) of 5.96 mm, average outer diameter (D) of 48.55, and average thickness ($2h$) of 1.38 mm were molded. The filling time of the part was approximately 1 s and the injection pressure was estimated to be 20 MPa. The material parameters were determined from steady shear and start-up of shear experiments [3]. Over a wide range of shear rates the PBT matrix behaves like a Newtonian fluid with viscosity η = 350 Pa·s. The coefficients were determined as α = 0.40, $\nu\zeta_{str}$ = 7417 Pa and $C_I = 0.02^2$. The weighted average length of the fiber was 364μm.

The initial orientation of the fibers was experimentally determined at the gate using method of ellipses [4] with several modifications to obtain unambiguous orientation measured over small sampling region. The specimen was metallographically polished in r,z-planes, plasma etched , and gold sputtered. A single-column of images were taken using reflective optical microscopy (20X) with a motorized stage. The images were stitched and the ϕ and θ were obtained using an in-house program written in Matlab. Then, the $\mathbf{A}$ was computed using Eq (6). The samples were cut along a line of constant θ. For validation purposes the orientation was determined in a similar manner along the gapwise direction at 10%, 40% and 90% of (R-r_i).

The filling of a disk having the characteristic values described above was simulated. The standard Galerkin method (GFEM) is used in the discretization of the HS flow approximation of the balance equations. The discontinuous Galerkin method (DGFEM) with a standard explicit Euler scheme is used to discretize the evolution equations. In the simulations only the top half of the domain was considered with no slip velocity at the wall and symmetry boundary conditions at z=0.

Results and Discussion

Experimental orientation

There are a limited number of studies which include both experimental and numerical work, therefore the initial conditions of orientation have typically been assumed as random orientation, especially for a center-gated disk [5]. Figure 1 and 2 respectively illustrate the diagonal and off-diagonal components of orientation determined experimentally from a 75% short shot center-gated disk. The asymmetric profile seen in A_{rr} along the cavity thickness at the gate region corroborates predictions indicted in the literature but never validated [6, 7]. Two plateaus with different values of A_{rr} can be seen in Fig. 1 indicating different levels of orientation with respect to the main flow direction for the upper half cavity and the lower half cavity. The higher values of A_{rr} in the upper half cavity have been attributed to higher velocity in the flow direction in the upper half [6, 7]. However, these experimental results add two observations not indicated before in the literature. Firstly, the orientation at the gate region becomes almost immediately planar orientation as seen from the values of $A_{zz} \approx 0$. Secondly, there is a cavity-wise asymmetry in $A_{r\theta}$, while the rest of the off diagonal

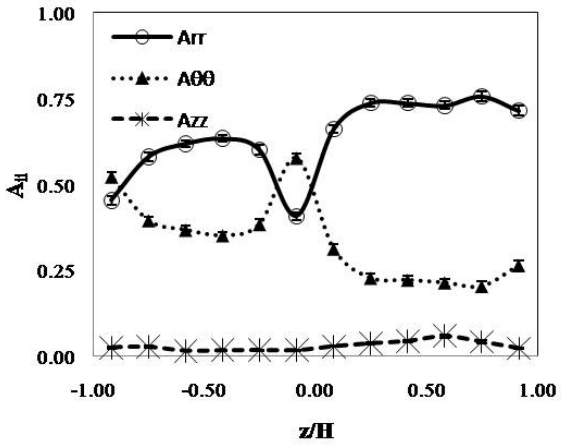

Figure 1. Experimental values of the diagonal components of **A** at the gate region. The symbols○, ▲, and * represent the A_{rr}, $A_{\theta\theta}$, and A_{zz}, respectively.

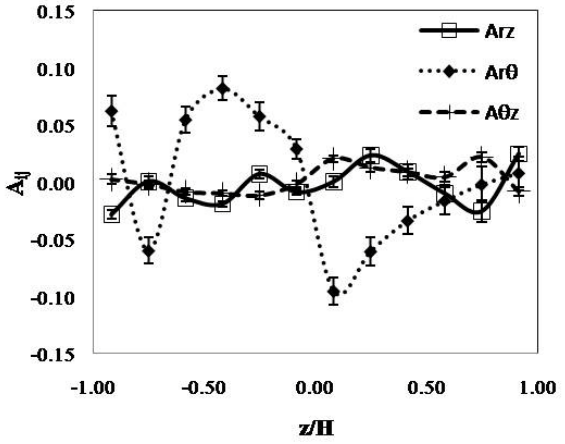

Figure 2. Experimental values of the off-diagonal components of **A** at the gate region. The symbols□, ♦, and + represent the A_{rz}, $A_{r\theta}$, and $A_{\theta z}$, respectively.

components remain close to 0, as seen in Fig. 2. Values of off-diagonal components close to 0, indicate tilt of fibers in 2 opposite directions that when approximately equal averaged make $A_{ij} \approx 0$. However, the $A_{r\theta}$ seen in Fig. 2 shows several regions along the thickness with a local tilt.

Orientation along the thickness measured at 40% and 90% (R-r_i) for PBT filled with short glass fibers indicate changes in the magnitude and distribution of the orientation components compared to the initial orientation at the gate. The initial asymmetry fades as a function of the radial location. However, experimental results suggest development of a symmetric orientation or stable structure of orientation for disks at r≥ 40% R as postulated by Rao and Altan [8]. Therefore, this observation suggests the formation of a secondary structure of orientation different from the accepted layered structure. This additional structure which evolves from the gate to about 40%R along the flow direction has not been previously reported. The impact of this structure on the mechanical properties can be critical to determine areas of weakness around the gate for large parts, especially when they have multiple gates.

Prediction of orientation

The experimental orientation in the 3 characteristic regions of flow of the center gated disk, i.e. entry, lubrication, and front were compared with results from standard commercial simulations and the proposed approach. The standard method of simulation is described by Folgar-Tucker model (α = 1), decoupled simulations, and random orientation at the gate while, the proposed approached is described by delayed Folgar Tucker (α = 0.4), coupled simulation, and experimentally measured orientation at the gate. Fig. 3 illustrates contrast in the cavity-wise A_{rr} orientation profile at a radial location in the entry region (10% (R-r_i)) between experimental results, standard and proposed approach. The generalized reduction in A_{rr} around the midplane (z/H=0) at entry region causes an asymmetric expansion of the core probably caused by a strong extensional flow in this area [9]. In this region, the standard and proposed approach fails to reproduce the experimental behavior. However, the asymmetry in the profile is still seen in the proposed approach, but with the minimum A_{rr} located in the lower half cavity. The orientation close to the wall can not be reproduced by both simulation approaches.

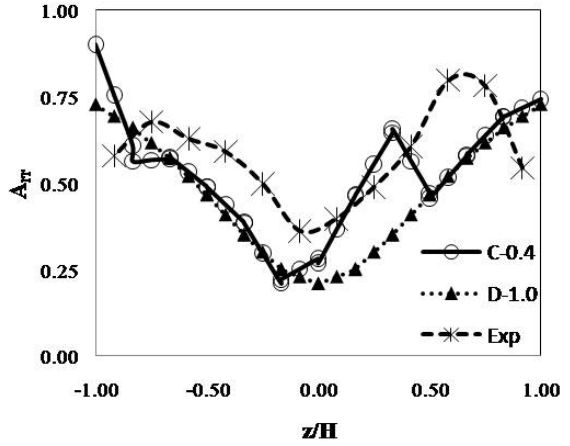

Figure 3. Experimental values of A_{rr} orientation component at the entry region (10% of radial flow length) (*) with the predicted values of A_{rr} orientation component using coupled simulation with measured orientation at the gate (○) and decoupled simulation with measured random orientation at the gate (▲).

Figure 4 shows the A_{rr} at a radial location in the lubrication region. The experimental orientation shows almost a symmetrical profile of orientation with a maximum A_{rr} = 0.88 for the upper and lower half of the cavity. Now the standard approach is capable of reproducing the orientation in the large portion of the core and transition layer, but fails in the shell layer. The proposed approach under-estimates the complete orientation profile and some asymmetry. The maximum A_{rr} for both simulations is found in plateau next to the wall, having a value of 0.83.

The A_{rr} orientation profile at a region close to the front is shown in Fig. 6. The experimental orientation profile shows a symmetrical behavior for the core and transition layer. However a large difference is seen in the upper and lower shell layers. The upper shell show a generalized reduction in orientation towards z/H = 0.75, not seen in other radial locations while the lower shell shows a constant value. At this location the maximum A_{rr} is found close to the walls, but in general the magnitude of A_{rr} is lower than the magnitudes found in the lubrication region. When the simulations are compared with the experimental values, the standard approach over predicts A_{rr} in the complete profile. The proposed approach become completely symmetric, and overlaps the results of the standard approach for the transition and shell layers. However, this is the only approach capable to reproduce a portion of the core region at a radial location close to the end-of-fill.

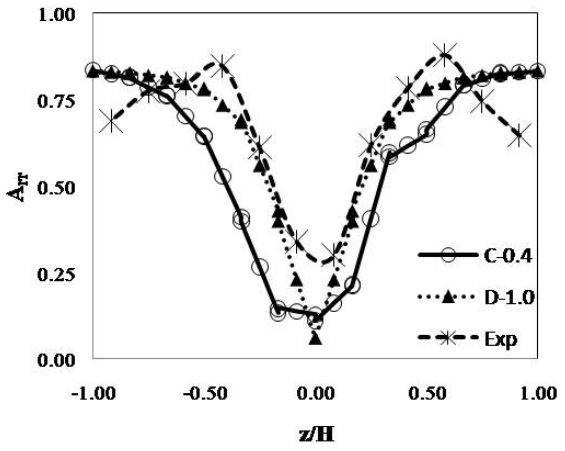

Figure 4. Experimental values of A_{rr} orientation component at the lubrication region (40% of radial flow length) (*) with the predicted values of A_{rr} orientation component using coupled simulation with measured orientation at the gate (○) and decoupled simulation with measured random orientation at the gate (▲).

The complete frontal region was qualitatively inspected to find reasons for the irregular behavior seen in the shell layer. The images of the advancing front (Fig 6) showed an irregular surface which is almost parabolic in shape. This region is severely affected by void spaces which are mainly found close to the free surface. The upper portion of the advancing front showed higher concentration of void spaces and a different structure of orientation when compared with the lower portion. Most of the fibers at the center of the advancing front seem to be oriented in θ-direction. However there is a tendency to have large amount of fiber aligning parallel to the flow in the upper but it rapidly goes down towards z/H=0. Therefore, the difference in dispersion of void spaces and fiber orientation at the front can be responsible for the irregular profile seen in the shell layer at a radial location close to the front.

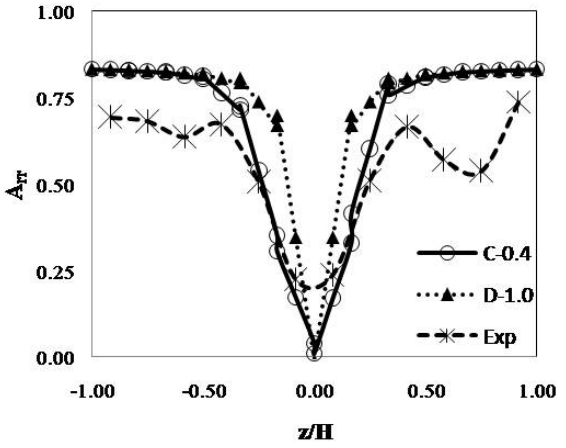

Figure 5. Experimental values of A_{rr} orientation component at a region close to the end-of-fill (90% of radial flow length) (*) with the predicted values of A_{rr} orientation component using coupled simulation with measured orientation at the gate (○) and decoupled simulation with measured random orientation at the gate (▲).

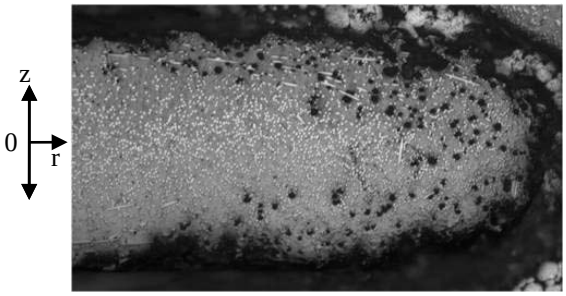

Fig 6. Reflective optical microscopy image (5X) of advancing front of PBT matrix with 30wt% short glass fibers.

Conclusion

The experimental results indicate that the profile of orientation at the gate was asymmetric and evolved into a steady layered structure of orientation at a radial location larger than 40% of the flow length. This suggests that the typical assumption of initial orientation as a symmetric random profile is not very accurate for a center-gated disk. An asymmetric profile was also found in the $A_{r\theta}$ component at the gate. The advancing front causes a reduction in A_{rr} at radial location of the end-of fill and distortions in the profile at the shell layers.

The use of model parameters, determined independently from the geometry, and a coupled fiber and orientation scheme help to delay the evolution of A_{rr} component of fiber orientation compared to the decoupled scheme typically assumed in existing literature. The proposed method delays too much the evolution of A_{rr} causing under estimation of A_{rr} at the entry and lubrication. However, the proposed method was able to reproduce the washout of asymmetric orientation profile observed experimentally. The standard approach was able to reproduce values of A_{rr} at the core and transition layers in the lubrication region. Experimental values of A_{rr} in core layer in a region close to the front were captured well by the proposed method. Many of the experimental observations were satisfactorily captured by the proposed model. However some additional modifications must be included in the proposed method to locally increase or reduce the predicted A_{rr}.

Acknowledgements

The financial support of NSF/DOE: DMI-052918 is gratefully acknowledged. Gregorio M. Vélez-García also acknowledges support from the NSF-MS&IE-IGERT and from the University of Puerto Rico-Mayagüez.

References

1. F. P. Folgar and C. L. Tucker, *J Reinf Plast Comp* **3**, 98-119 (1984).
2. A. Eberle, et al, *J Non-Newtonian Fluid Mech* **165**, 110-119 (2002)..
3. A. Eberle, et al, *J Rheol* **53**, 1049-1068 (2009).
4. A. R. Clarke and C. N. Eberhadt. Microscopy techniques for materials science. CRC (2002).
5. R. S. Bay and C. L. Tucker, *Polym Comp* **13**, 332-341 (1992).
6. B. E. VerWeyst and C. L. Tucker, *Can J Chem Eng* **80**, 1093-1106 (2002).
7. D. H. Chung and T. H. Kwon, *J Non-Newtonian Fluid Mech* **107**, 67-96 (2002).
8. B. N. Rao and M. C. Altan, *J Rheol* **39**, 581-599 (1995).
9. S. Ranganathan and S. G. Advani, *J Non-Newtonian Fluid Mech* **47**, 107-136 (1993).